



HAL
open science

Estimation of synchronous machine parameters by standstill tests

Mourad Hasni, Omar Touhami, Rachid Ibtouen, Maurice Fadel, Stéphane
Caux

► **To cite this version:**

Mourad Hasni, Omar Touhami, Rachid Ibtouen, Maurice Fadel, Stéphane Caux. Estimation of synchronous machine parameters by standstill tests. *Mathematics and Computers in Simulation*, 2010, 81 (2), pp.277-289. 10.1016/j.matcom.2010.05.010 . hal-03574285

HAL Id: hal-03574285

<https://ut3-toulouseinp.hal.science/hal-03574285>

Submitted on 15 Feb 2022

HAL is a multi-disciplinary open access archive for the deposit and dissemination of scientific research documents, whether they are published or not. The documents may come from teaching and research institutions in France or abroad, or from public or private research centers.

L'archive ouverte pluridisciplinaire **HAL**, est destinée au dépôt et à la diffusion de documents scientifiques de niveau recherche, publiés ou non, émanant des établissements d'enseignement et de recherche français ou étrangers, des laboratoires publics ou privés.

Estimation of synchronous machine parameters by standstill tests

M. Hasni^{a,*}, O. Touhami^a, R. Ibtouen^a, M. Fadel^b, S. Caux^b

^a *Laboratoire de Recherche en Electrotechnique – Ecole Nationale Polytechnique 10, Av. Pasteur, El Harrach, Bp. 182, 16200 Algiers, Algeria*

^b *Laboratoire Plasma et Conversion d'Energie - Unité mixte CNRS-INP Toulouse, 2, rue Camichel, BP 7122, 31071 Toulouse Cedex 7, France*

Abstract

In this paper we present the results of a time-domain identification procedure to estimate the linear parameters of a salient-pole synchronous machine at standstill.

A new approach is proposed for the estimation of synchronous machine coupled to DC-chopper and Pseudo Random Binary Sequences excitations; using data recorded during steady-state operation of the chopper-machine unit. This procedure consists of defining and conducting the standstill tests, identifying the model structure, estimating the corresponding parameters, and validating the resulting model. The signals used for identification are the different excitation voltages at standstill and the flowing current in different windings. We estimate the parameters of operational impedances, or in other terms, the reactances and the time constants.

The results are presented from tests on a synchronous machine of 3 kVA/220 V/1500 rpm.

Keywords: Synchronous machine; Parameter estimation; Standstill tests

1. Introduction

There are many suggested methods for the determination of synchronous machine parameters. Among the modern techniques used are neural networks, finite elements, on-line and off-line statistical methods, frequency response, load rejection and others [3,5,8,12–14].

Different measurement techniques, identification procedures and models structures are developed to obtain models as accurate predictors for the transient behaviour of generators.

The standstill modelling approach has received great emphasis due to its relatively simple testing method where the d - and q -axis are decoupled [2,6,10,14,15].

This paper deals with the experimental determination of synchronous machine parameters and models.

The characteristic parameters obtained from reduced models of the synchronous machine are proposed and there is no need to any hypothesis. The first order equations, which approximate all the behaviour of the machine, are given. These reduced models traduce the subtransient, the transient and the steady-state operations of the machine respectively.

Nomenclature

List of symbols

p	Laplace's operator
ω, ω_0	angular speeds
φ_d, φ_q	d - and q -axis flux linkage
V_d, V_q	d - and q -axis stator voltages
i_d, i_q	d - and q -axis stator currents
V_f, i_f	d -axis field voltage and current
r_a, r_f	armature and field resistances
x_d, x_q	d - and q -axis synchronous reactance
x_d', x_d''	d -axis transient and subtransient reactances
x_q', x_q''	q -axis transient and subtransient reactances
x_{md}	d -axis magnetizing reactance
x_a	armature leakage reactance
x_f	field leakage reactance
$Y_{d,q}(p)$	d - and q -axis operational admittances
T_{fo}, T_f	field open-circuit and short-circuit time constant
T_{do}', T_d'	d -axis transient open-circuit and short-circuit time constant
T_{do}'', T_d''	d -axis subtransient open-circuit and short-circuit time constant
T_{qo}', T_q'	q -axis transient open-circuit and short-circuit time constant
T_{qo}'', T_q''	q -axis subtransient open-circuit and short-circuit time constant
PRBS	Pseudo Random Binary Sequences

Depending on whether the synchronous machine is supplied with voltage, we propose different differential equations from which analytical expressions of the currents and the voltages are deduced. The expressions are given as functions of the characteristic parameters: open-circuit and short-circuit time constants and reactances.

As an application, we have worked on the following methods:

- DC decay test in armature winding at standstill.
- Excitation by DC-chopper.
- Excitation by PRBS.

The purpose of these studies is to determine the static experimental conditions to estimate the parameters of a salient-pole synchronous machine using DC decay, DC-chopper and Pseudo Random Binary Sequences excitations.

The tests are performed and studied on a synchronous machine ($S_n = 3$ kVA, $U_n = 220$ V, $I_n = 8$ A, $N_n = 1500$ rpm).

2. Synchronous machine modelling

The study of the electric machines based on the Park's transform was already treated in several works and specialized publications. This model allows, by a change of reference frame, to pass from the stator system to the rotor system with elimination of certain variables.

The basic model consists to considering one salient-pole synchronous machine with one pair of poles to the rotor and a three-phase stator winding.

The field winding is on the rotor of the machine according to the axis of the salience (direct axis).

The presence of grid or cage of dampers to the rotor, are modeled by two equivalent circuits dampers; one on the direct axis and the other on the quadrature axis.

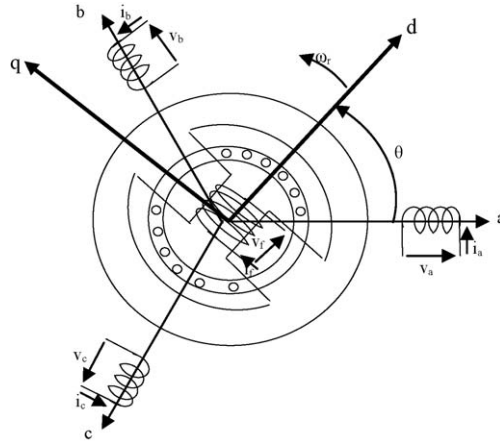


Fig. 1. Three-phase synchronous machine with dampers.

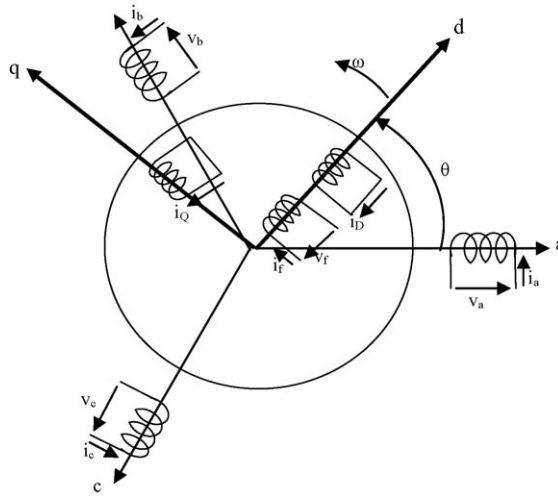


Fig. 2. Three-phase synchronous machine, dampers assimilated to two windings in short-circuit

The six windings representing Fig. 1 are described by the following equations

$$\left. \begin{aligned} V_a &= R_a i_a + \frac{d\varphi_a}{dt} \\ V_b &= R_a i_b + \frac{d\varphi_b}{dt} \\ V_c &= R_a i_c + \frac{d\varphi_c}{dt} \end{aligned} \right\} \text{armature (Stator)} \quad (1)$$

$$\left. \begin{aligned} V_f &= R_f i_f + \frac{d\varphi_f}{dt} \\ 0 &= R_D i_D + \frac{d\varphi_D}{dt} \\ 0 &= R_Q i_Q + \frac{d\varphi_Q}{dt} \end{aligned} \right\} \text{field (Rotor)} \quad (2)$$

The voltage applied to the D and Q circuits are null, since they are in short-circuit (Fig. 2).

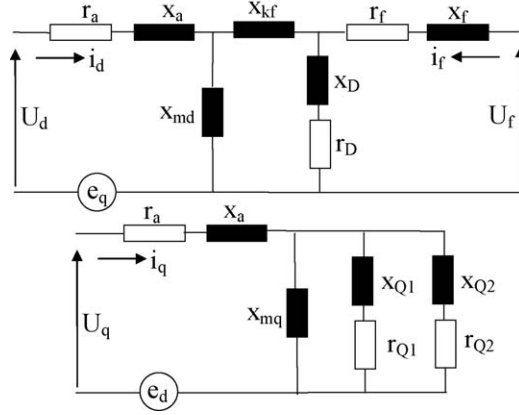


Fig. 3. Standard d - q axis circuit models.

2.1. Choice of model's order

Using the Park's d and q -axis reference frame, the synchronous machine is supposed to be modelled with one damper winding for the d -axis and two windings for the q -axis (2×2 model) as shown in Fig. 1 [1,7,8,14,15].

Damper circuits, especially those in the quadrature axis provide much of the damper torque. This particularly important in studies of small signal stability where conditions are examined about some operating point [13]. The second order direct axis models includes a differential leakage reactance. In certain situations for second order models, the identity of the transients field winding. Alternatively, the field circuit topology can alter by the presence of an excitation system, with its associated non-linear features.

By considering Fig. 3, the equations of the machine are:

- Voltage equations

$$V_d(p) = r_a i_d(p) + p\varphi_d(p) + \omega_r \varphi_q(p) \quad (3)$$

$$V_q(p) = r_a i_q(p) + p\varphi_q(p) - \omega_r \varphi_d(p) \quad (4)$$

$$V_f(p) = r_f i_f(p) + p\varphi_f(p) \quad (5)$$

$$0 = r_D i_D(p) + p\varphi_D(p) \quad (6)$$

$$0 = r_Q i_Q(p) + p\varphi_Q(p) \quad (7)$$

After eliminating φ_f , i_f , φ_D , i_D , φ_Q , i_Q we obtains the following equations:

$$V_d(p) = r_a i_d(p) + p\varphi_d(p) + \omega_r \varphi_q(p) \quad (8)$$

$$V_q(p) = r_a i_q(p) + p\varphi_q(p) - \omega_r \varphi_d(p) \quad (9)$$

$$\varphi_d(p) = X_d(p) i_d(p) + G(p) V_f(p) \quad (10)$$

$$\varphi_q(p) = X_q(p) i_q(p) \quad (11)$$

This writing form of the equations of the machine has the advantage of being independent of the number of dampers considered on each axis.

In fact, it is the order of the functions $X_{d,q}(p)$ and $G(p)$, which depend on the number of dampers.

For a machine at standstill, the rotor speed is zero ($w=0$) and using the p Laplace operator, the voltage equations can then be written as:

- For the d -axis

$$V_d = \left[r_a + \frac{P}{\omega_0} X_d(p) \right] i_d + pG(p) v_f \quad (12)$$

$$V_f = \left[r_f + \frac{p}{\omega_0} X_f(p) \right] i_f + \frac{p}{\omega_0} X_{md} i_d \quad (13)$$

- For the q -axis

$$V_q = \left[r_a + \frac{p}{\omega_0} X_q(p) \right] i_q \quad (14)$$

with the operational reactances:

$$X_{d,q,f}(p) = X_{d,q,f} \frac{(1 + pT_{d,q,f}')(1 + pT_{d,q,f}'')}{(1 + pT_{d0,q0,f0}')(1 + pT_{d0,q0,f0}'')} \quad (15)$$

and the operational function $G(p)$:

$$G(p) = \frac{X_{md}}{r_f} \frac{1}{1 + pT_{d0}'} \quad (16)$$

where d , q , f denote the d -axis, q -axis and field respectively. From these equations, it follows that only the three functions $X_d(p)$, $X_q(p)$ and $G(p)$ are necessary to identify a synchronous machine.

The reduced operational admittances of the d -axis and q -axis are deduced from the input–output signals

$$Y_{d,q}(p) = \frac{i_{d,q}(p)}{V_{d,q}(p)},$$

or in other terms

$$Y_{d,q}(p) = \frac{1 + p(T_{d0,q0}' + T_{d0,q0}'') + p^2 T_{d0,q0}' T_{d0,q0}''}{r_a + p \left[r_a (T_{d0,q0}' + T_{d0,q0}'') + \frac{x_{d,q}}{\omega_0} \right] + p^2 \left[r_a T_{d0}' T_{d0}'' + \frac{x_{d,q}}{\omega_0} (T_{d,q}' + T_{d,q}'') \right] + p^3 \frac{x_d}{\omega_0} T_{d,q}' T_{d,q}''} \quad (17)$$

The reduced operational admittances take the following forms

$$H_{d,q}(p) = \frac{b_0 + b_1 p + b_2 p^2}{1 + a_1 p + a_2 p^2 + a_3 p^3} \quad (18)$$

The problem lies in calculating the constants a_1 , a_2 , a_3 , b_0 , b_1 and b_2 by using non-linear programming methods. For this purpose we have used a program, which calculates the six parameters quoted above from the input-output signals for each axis. The structure of the model being selected, then the form of the transfer function is known, thus the order of the numerator and of the denominator of equation (18) are, for our case, $n=2$ and $m=3$.

The objective of our estimation task is to make the simulated model response matches that of the actual response by minimizing the error between the two of themes. In order to minimize this error, a good optimisation technique is needed. For that we used a quadratic criterion to quantify the difference between the process and the model which is based on the Levenberg–Marquardt algorithm.

2.2. Levenberg–Marquardt's algorithm

The Levenberg–Marquardt algorithm [11] is a general non-linear downhill minimisation algorithm. It dynamically mixes Gauss-Newton and gradient-descent iterations. The unknown parameters are represented by the vector x , and let the noisy measurements of x be made:

$$z(j) = h(j; x) + w(j), \quad j = 1, \dots, k \quad (19)$$

where $h(j)$ is a measurement function and $w(j)$ is a zero-mean noise with covariance $N(j)$. Since we are describing an iterative minimization algorithm, we shall assume that we have an estimate \hat{x}^- of x . A new estimate \hat{x} maximizes

$$\chi^2(\hat{x}) = \sum_{j=1}^k (z(j) - h(j; \hat{x}))^T N(j)^{-1} (z(j) - h(j; \hat{x})) \quad (20)$$

We form a quadratic approximation to $\chi^2(\cdot)$ around \hat{x}^- , and minimize this approximation to $\chi^2(\cdot)$ to obtain a new estimate \hat{x}^+ . In general we can write such a quadratic approximation as

$$\chi^2(x) \approx \alpha - 2a^T(x - \hat{x}^-) + (x - \hat{x}^-)^T A(x - \hat{x}^-)$$

for scalar α , vector a and matrix A .

After differentiating we obtain $\partial\chi^2/\partial x = -2a + 2A(x - \hat{x}^-)$, $\partial^2\chi^2/\partial x^2 = 2A$.

At the minimum point, \hat{x} we have $\partial\chi^2/\partial x = 0$. This means that

$$A(\hat{x}^+ - \hat{x}^-) = a. \quad (21)$$

Thus we need to obtain a and A to compute the update. We now consider the form of $\chi^2(\cdot)$ in (20). Writing the Jacobian of $h(j, x)$ as $H(j) = \partial h(j)/\partial x$, we have

$$\frac{\partial\chi^2}{\partial x} = -2 \sum_{j=1}^k H(j)^T N(j)^{-1} (z(j) - h(j; x)), \quad (22)$$

$$\frac{\partial^2\chi^2}{\partial x^2} = 2 \sum_{j=1}^k H(j)^T N(j)^{-1} H(j) - 2 \sum_{j=1}^k \left(\frac{\partial H(j)}{\partial x} \right)^T N(j)^{-1} (z(j) - h(j; x)) \approx 2 \sum_{j=1}^k H(j)^T N(j)^{-1} H(j), \quad (23)$$

In the last formula for $\partial^2\chi^2/\partial x^2$, the terms involving the second derivatives of $h(j, \cdot)$ have been omitted. This is done because these terms are generally much smaller and can in practice be omitted.

Now we solve the above equations for a and A given the values of the function $h(j)$ and the Jacobian $H(j)$ evaluated at the previous estimate \hat{x}^- . We have immediately $A = \sum_{j=1}^k H(j)^T N(j)^{-1} H(j)$.

We now write the innovation vectors $v(j)$ as

$$v(j) = z(j) - h(j; \hat{x}^-)$$

Then we have

$$a = \sum_{j=1}^k H(j)^T N(j)^{-1} v(j) \quad (24)$$

Combining Eqs. (21) and (24) we obtain the linear system

$$A(\hat{x}^+ - \hat{x}^-) = a = \sum_{j=1}^k H(j)^T N(j)^{-1} v(j) \quad (25)$$

To be solved for the adjustment $\hat{x}^+ - \hat{x}^-$, the covariance of the state is $P = A^{-1}$.

The update (25) may be repeated, substituting the new \hat{x}^+ as \hat{x}^- , and improving the estimate until convergence is achieved according to some criterion. Levenberg–Marquardt modifies this updating procedure by adding a parameter λ to the diagonal elements of the linear system matrix before inverting it to obtain the update. λ is reduced if the last iteration gave an improved estimate, i.e. if χ^2 was reduced, and increased if J increased, in which case the estimate of x is reset to the estimate before the last iteration.

3. Standstill tests

In this section, the practical aspects of measurements are described and synchronous machine conditions for standstill time-domain data are given [1,4,9,12].

Fig. 4 shows the experimental procedure of identification.

The alignment of the rotor can be accomplished with short-circuited field winding. A sinusoidal voltage is applied between two stator phases. The duration of the application of the voltage should be limited to avoid serious overheating of solid parts. The rotor is slowly rotated to find the angular positions corresponding to the maximum value of the excitation current that gives the direct axis and zero value of the excitation winding current that corresponds to the quadrature axis.

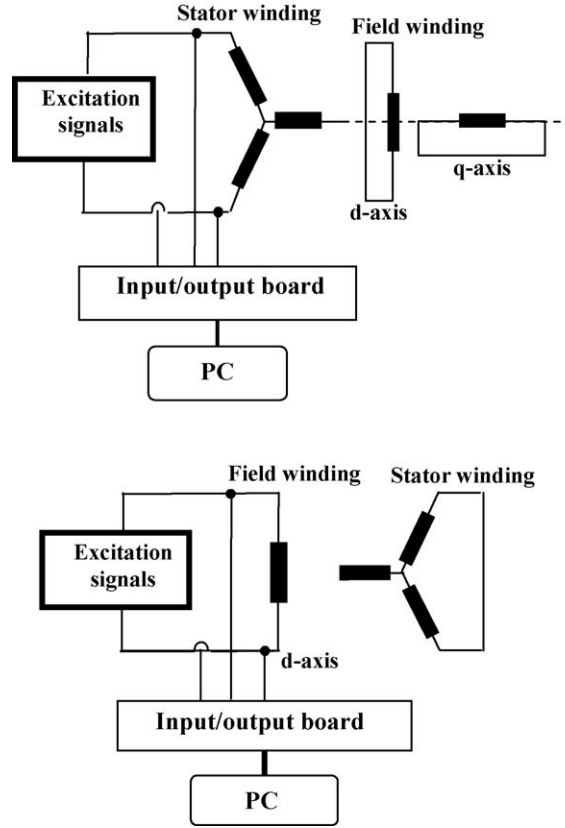


Fig. 4. Experimental procedure of identification.

The machine is not saturated during standstill tests; in fact, the flux densities are below those on the more linear part of the permeability characteristic that is commonly referred to as “unsaturated”. The determination of the quantities referred to as the unsaturated state of the machine must be done from tests, with supply voltages (1–2%) of the nominal values.

3.1. Experimental procedure

The two principal characteristic parameters, which relate to the listed definitions, are:

- $Z_d(p)$: the direct axis operational impedance equal to $r_a + pl_d(p)$, where r_a is the DC armature resistance per phase.
- $Z_q(p)$: the quadrature axis operational impedance equal to $r_a + pl_q(p)$.

The above two quantities are the stator driving point impedances. While the above quantities are consistent with the definitions, an alternative method of measuring these parameters is given as follow:

$$G(p) = \frac{I_{fd}(p)}{pI_d(p)} \quad \text{for } E_{fd} = 0 \quad (26)$$

With a shorted field winding ($V_f = 0$), the d - and q -axis operational admittances are given:

$$Y_{d,q}(p) = \frac{i_{d,q}(p)}{v_{d,q}(p)} \quad \text{for } V_f = 0 \quad (27)$$

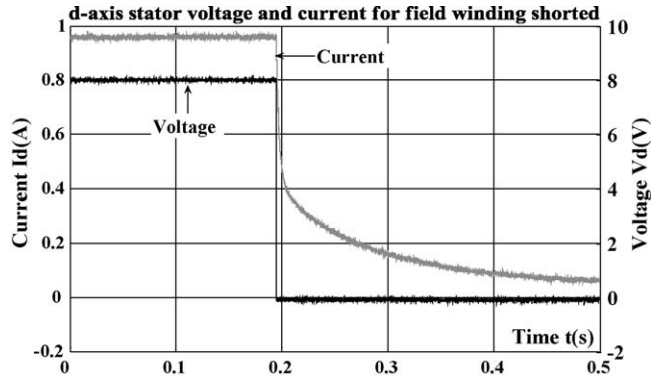


Fig. 5. *d*-Axis stator voltage and current for field winding shorted.

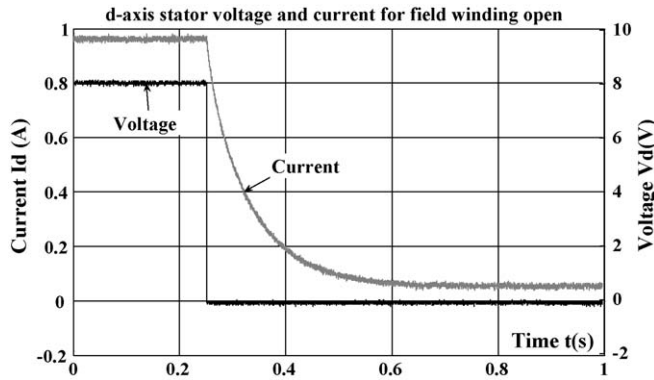


Fig. 6. *d*-Axis stator voltage and current for field winding open.

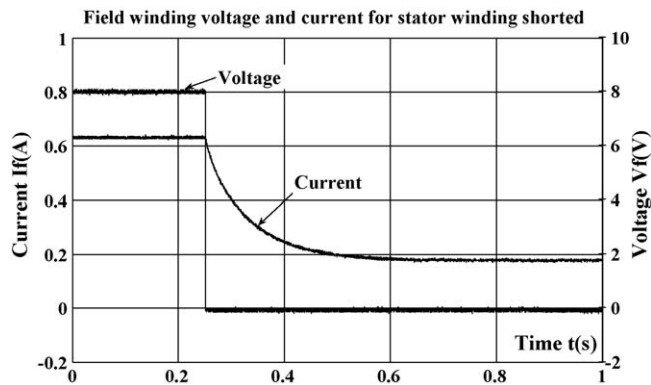


Fig. 7. Field voltage and current for stator winding shorted.

With a *d*-axis armature shorted ($V_d = 0$), the field winding parameters can be obtained by:

$$Y_f(p) = \frac{i_f(p)}{v_f(p)} \quad \text{for } V_d = 0 \quad (28)$$

The waveforms recorded for the various excitations used are shown in Figs. 5–13.

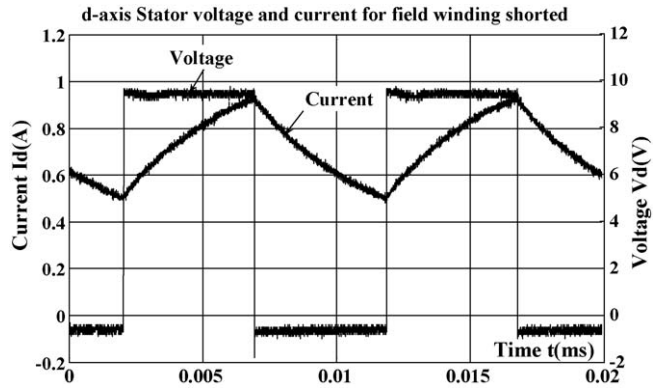


Fig. 8. *d*-Axis stator voltage and current for field winding shorted.

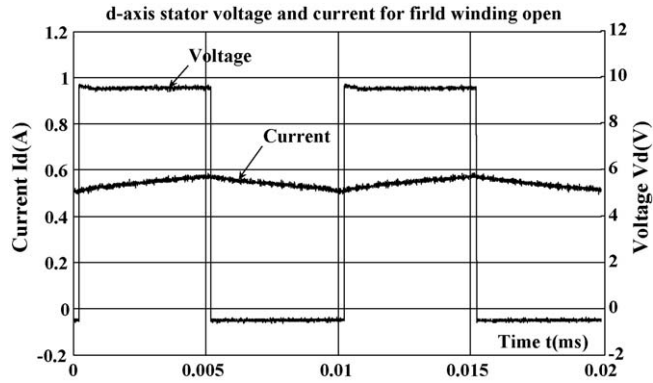


Fig. 9. *d*-Axis stator voltage and current for field winding open.

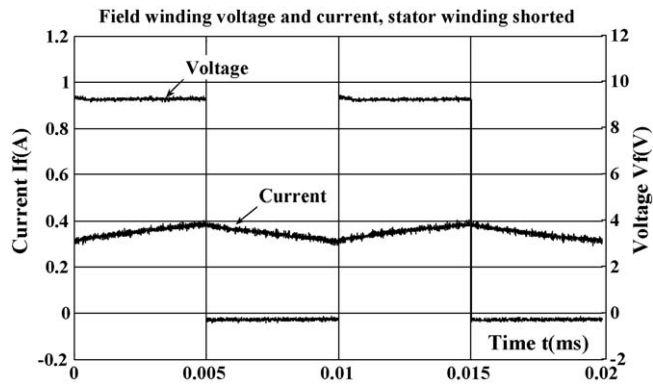


Fig. 10. Field voltage and current for stator winding shorted.

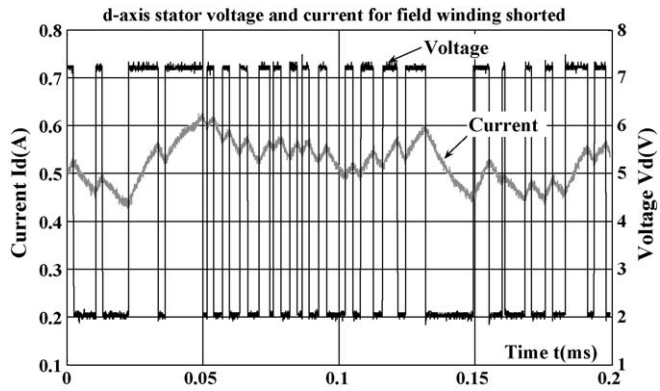


Fig. 11. *d*-Axis stator voltage and current for field winding shorted.

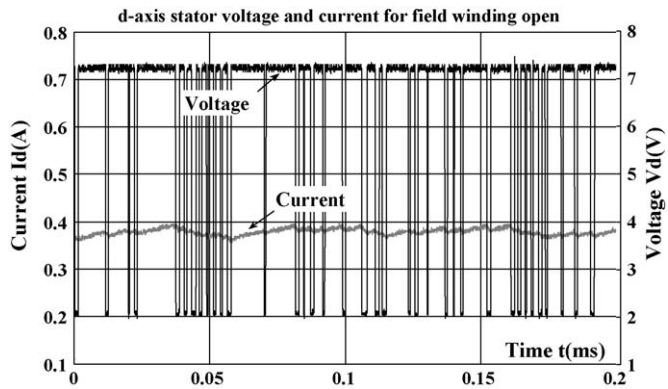


Fig. 12. *d*-Axis stator voltage and current for field winding open.

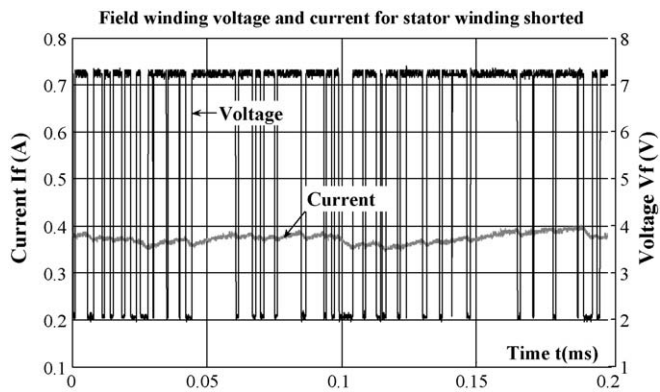


Fig. 13. Field voltage and current for stator winding shorted.

Table 1
Identified synchronous machine parameters.

Parameters	DC-chopper	PRBS voltages	DC decay
R_a (p.u.)	0.149	0.149	0.149
R_f (p.u.)	4.95	4.95	4.95
T_d' (s)	0.1856	0.1675	0.1840
T_d'' (s)	0.0490	0.0526	–
T_{d0}' (s)	1.0907	0.9189	1.1346
T_{d0}'' (s)	0.4350	0.4785	–
T_q' (s)	0.1476	0.1284	0.1509
T_q'' (s)	0.0461	0.0361	–
T_{q0}' (s)	0.9022	0.7849	1.0279
T_{q0}'' (s)	0.4631	0.3829	–
T_f' (s)	0.2205	0.2306	0.2185
X_f (p.u.)	0.5314	0.5438	0.5287
X_d (p.u.)	2.0667	1.9980	2.0515
X_d' (p.u.)	0.3516	0.3459	0.3758
X_q (p.u.)	1.3378	1.5639	1.3880
X_q' (p.u.)	0.2089	0.1904	0.2413
X_d'' (p.u.)	0.0396	0.0345	–
X_q'' (p.u.)	0.0218	0.0198	–

3.2. DC decay test

Figs. 5 and 6 show the current and voltage waveforms during the DC decay test, for the d -axis tests (field winding shorted and open, respectively). Fig. 7 shows field voltage and current for stator winding shorted.

3.3. Excitation by DC-chopper

In the same way, Figs. 8 and 9 show the current and voltage waveforms during the DC-chopper test, for the d -axis tests (field winding shorted and open respectively). Fig. 10 shows field voltage and current for stator winding shorted.

3.4. Excitation by PRBS

Figs. 11 and 12 show the current and voltage waveform during the Pseudo Random Binary Sequences excitation test, for the d -axis tests (field winding shorted and open, respectively). Fig. 13 shows field voltage and current for stator winding shorted.

4. Identification results

The parameters identified by using the various excitations signals are gathered in Table 1.

The time-domain approach offers a method, which can yield useful models, particularly in the data, is interpreted correctly.

The proposed model, the quality and the experimental data used to identify the model parameters and the robustness of the estimation technique, affects the fidelity of synchronous machine models.

The results obtained with the various excitations and by using the same procedure of identification, show a good agreement between the various identified parameters. It should be noted that the various signals used made it possible to determine all the parameters of the equivalent circuits, except for the dc decay test which does not enable us to determine the parameters varying very fast.

5. Model validation

The identified d - q axis models are verified by comparing their simulated d - q axis stator currents responses against the measured standstill response, for that we present in Fig. 14, simulation results for d -axis stator current for signals among

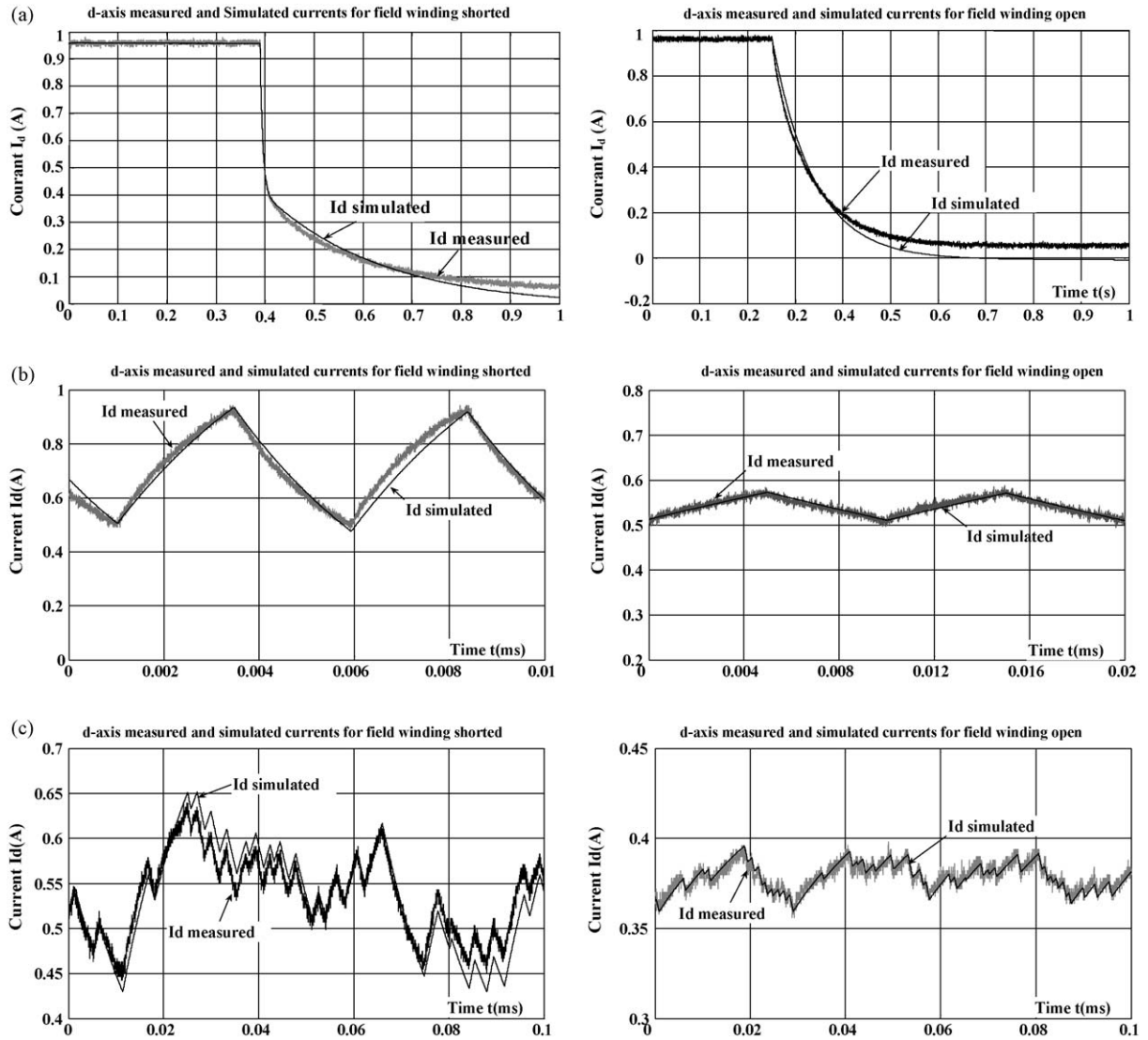


Fig. 14. (a) Comparison between measured and simulated d -axis current, for field winding open and short circuited (excitation by DC decay). (b) Comparison between measured and simulated d -axis current, for field winding open and short circuited (excitation by DC-chopper voltages). (c) Comparison between measured and simulated d -axis current, for field winding open and short circuited (excitation by PRBS voltages).

those presented previously. The measured and simulated responses to off-line excitation disturbances comparison show that the machine linear parameters are accurately estimated to represent the machine at standstill conditions.

6. Conclusion

This paper presents a step-by-step procedure to identify the parameter values of the d - q axis synchronous machine models using the standstill time-domain data analysis.

A three-phase salient-pole laboratory machine rated 3 kVA and 220 V is tested at standstill and its parameters are estimated. Both the model transfer function and the equivalent circuit model parameters are identified using the Levenberg–Marquardt algorithm.

The various excitations signals used gave very similar parameters results. Moreover, the simulation of measured and calculated parameters shows the validity of the results obtained. It should be noted that the various signals used

made it possible to determine all the parameters of the equivalent circuits, except for the DC decay test which does not enable us to determine the parameters very quickly varying.

Among the advantages claimed for the time-domain approach at standstill, is that the tests are safe and relatively inexpensive.

Furthermore, information about the quadrature axis, as well as the direct axis of the machine is obtained.

References

- [1] ANSI-IEEE Std.115, Test Procedures for Synchronous Machines, Part. I – Acceptance and Performance Testing, Part. II – Test Procedures and Parameter Determination for Dynamic Analysis, Approved, 1995.
- [2] E.C. Bortoni, J.A. Jardini, A standstill frequency response method for large salient pole synchronous machines, *IEEE Trans. Energy Convers.* 19 (2004) 687–691.
- [3] N. Dedene, R. Pintelon, P. Lataire, Estimation of a global synchronous machine model using a multiple input multiple output estimators, *IEEE Trans. Energy Convers.* 18 (2003) 11–16.
- [4] EPRI Report, Confirmation of Test Methods for Synchronous Machine Dynamic Performance Models, EPRI EL-5736, Project 2328-1, Final Report, 1987.
- [5] V. Graza, M. Biriescu, G. Liuba, V. Cretu, Experimental determination of synchronous machines reactance from DC decay at standstill, in: *IEEE Instrumentation and Measurement Technology Conference, Budapest, Hungary, 2001*, pp. 1954–1957.
- [6] M. Hasni, O. Touhami, R. Ibtouen, M. Fadel, Modelling, Identification of a synchronous machine by using singular perturbations, *Int. Rev. Electr. Eng.* (2006) 418–425.
- [7] M. Hasni, O. Touhami, R. Ibtouen, M. Fadel, S. Caux, Synchronous machine parameter estimation by standstill frequency response tests, *ICIT 2008*, in: *IEEE International Conference, Chengdu, China, 2008*, pp. 1–6.
- [8] S. Horning, A. Keyhani, I. Kamwa, On-line evaluation of a round rotor synchronous machine parameter set estimation from standstill time-domain data, *IEEE Trans. Energy Convers.* 12 (1997) 289–296.
- [9] IEC.34-4, Standard on Rotating Electrical Machines, Part 4, Methods for Determining Synchronous Machine Quantities from Tests, IEC Publication 34-4, 1985.
- [10] I. Kamwa, P. Viarouge, H. Le-Huy, J. Dickinson, Three transfer function approach building phenomenological models of synchronous machines, *IEE Proc-gener* 141 (1994) 89–98.
- [11] D.W. Marquardt, An algorithm for least-squares estimation of nonlinear parameters, *J. Soc. Ind. Appl. Math.* 11 (2) (1983) 431–441.
- [12] F.S. Sellschopp, M.A. Arjona, A tool for extracting synchronous machines parameters from the dc flux decay test, *Comp. Electr. Eng.* 31 (2005) 56–68.
- [13] O. Touhami, H. Guesbaoui, C. Jung, Synchronous machine parameter identification by a multi-time scale technique, *IEEE Trans. Ind. Appl.* 30 (1994) 1900–1908.
- [14] A. Tumageanian, A. Keyhani, Identification of synchronous machine linear parameters from standstill step voltage input data, *IEEE Trans. Energy Convers.* 10 (1995) 232–240.
- [15] L. Vicol, M. Tu Xuan, R. Wetter, J.-J. Simond, I.A. Viorel, On the Identification of the Synchronous Machine Parameters Using Standstill DC Decay Test, *ICEM, Chania, Crete Island, Greece, 2006*.